New Journal of Physics
The open access journal at the forefront of physics

Deutsche Physikalische Gesellschaft DPG IOP Institute of Physics

PAPER • OPEN ACCESS

Inhibition of spread of typical bipartite and genuine multiparty entanglement in response to disorder

To cite this article: George Biswas *et al* 2021 *New J. Phys.* **23** 113042

New Journal of Physics
The open access journal at the forefront of physics

Deutsche Physikalische Gesellschaft DPG
IOP Institute of Physics

Published in partnership with: Deutsche Physikalische Gesellschaft and the Institute of Physics

OPEN ACCESS

RECEIVED
22 May 2021

REVISED
28 October 2021

ACCEPTED FOR PUBLICATION
9 November 2021

PUBLISHED
25 November 2021

PAPER

Inhibition of spread of typical bipartite and genuine multiparty entanglement in response to disorder

George Biswas[1], Anindya Biswas[1] and Ujjwal Sen[2,*]

[1] Department of Physics, National Institute of Technology Sikkim, Ravangla, South Sikkim 737 139, India
[2] Harish-Chandra Research Institute, HBNI, Chhatnag Road, Jhunsi, Prayagraj 211 019, India
[*] Author to whom any correspondence should be addressed.

E-mail: ujjwal@hri.res.in

Keywords: typical entanglement, disorder-induced inhibition of spread, Gaussian disorder, non-Gaussian disorder

Abstract

The distribution of entanglement of typical multiparty quantum states is not uniform over the range of the measure utilized for quantifying the entanglement. We intend to find the response to disorder in the state parameters on this non-uniformity for typical states. We find that the typical entanglement, averaged over the disorder, is taken farther away from uniformity, as quantified by decreased standard deviation, in comparison to the clean case. The feature is seemingly generic, as we see it for Gaussian and non-Gaussian disorder distributions, for varying strengths of the disorder, and for disorder insertions in one and several state parameters. The non-Gaussian distributions considered are uniform and Cauchy–Lorentz. Two- and three-qubit pure state Haar-uniform generations are considered for the typical state productions. We also consider noisy versions of the initial states produced in the Haar-uniform generations. A genuine multiparty entanglement monotone is considered for the three-qubit case, while concurrence is used to measure two-qubit entanglement.

1. Introduction

Random numbers have useful applications in classical information theory, including in cryptography, stochastic estimations, etc. Random quantum states and random unitary operators are the quantum analogs of random numbers in quantum information theory [1–7]. Moreover, random states occur naturally when a quantum system gets measured in an unknown basis, or when the system is perturbed by an uncontrolled and unknown environment. Similarly, random states can also get generated in the initialization of the corresponding quantum devices. Quantum algorithms and other quantum-enabled protocols [8, 9] sometime assume that interaction with environment can somehow be avoided. However, unless an error-correction procedure [8, 9] is incorporated, which can be costly, random states would naturally appear and remain in the corresponding quantum circuits.

In this paper, we investigate entanglement properties [10–12] of randomly generated bipartite and tripartite pure and mixed quantum states, with and without disorder. The case without disorder has, e.g. been considered in [13–23]. We anticipate a situation where noise from the environment, during the preparation of the state for feeding a quantum circuit or during the evolution of the state through the circuit, gathers as disorder in the parameters of the state written as a superposition over the computational basis. Noise typically acts with a preferred basis, and we assume that basis in our case to be the computational basis, which in turn justifies the building up of disorder in the parameters of the state written in that basis. The random bipartite and tripartite states are chosen Haar uniformly. The disorder is inferred as quenched, and assumed to be spread according to Gaussian, uniform, or Cauchy–Lorentz distributions [24].

Quantum entanglement is the existence of states of several separated systems that cannot be created by only local quantum operations and classical communication (LOCC) between the systems [25–27]. There are a large number of measures of entanglement of both bipartite and multipartite quantum states.

However, not many of them are computable. We use the concurrence [28, 29] to measure bipartite entanglement and the computable entanglement monotone of Jungnitsch, Moroder, and Gühne (JMG) [30] for measuring genuine multiparticle entanglement. We find that the introduction of disorder in multiparty quantum state parameters generically inhibits the spread of average entanglement for typical states of the multiparty systems considered. The considerations are restricted to two- and three-qubit states, of both pure and noisy varieties.

The rest of the paper is arranged as follows. In section 2, we briefly discuss the generation of Haar uniform random states, the probability distributions corresponding to the disorders inserted, and the measures employed to compute quantum entanglement. A short discussion of disorder insertion and its averaging is also given there. Also present there is a brief discussion on skewness and kurtosis of a distribution. In section 3, we discuss the entanglement distributions obtained for bipartite and tripartite Haar-uniformly generated pure states, with and without disorder. Several cases are considered, and are given in separate subsections. Noisy versions of the input states are also used, that lead to mixed states, and these analyses appear in sections 3.2 and 3.6. A conclusion is presented in section 4.

2. Gathering the tools

2.1. Haar uniform random states and probability density functions

The multiparty states utilized for the computation of entanglement and average entanglement have been chosen 'Haar uniformly'. A pure quantum state can be written as

$$|\psi\rangle = \sum_{j=1}^{n} (c_{1j} + \mathrm{i}c_{2j})|j\rangle \tag{1}$$

where $|j\rangle$ represents the jth orthonormal basis vector in the n-dimensional Hilbert space, $\mathbb{C}^n$, and c_{1j}, c_{2j} are real numbers, constrained by the normalization condition, $\langle\psi|\psi\rangle = 1$. In particular, for an m-qubit system, $n = 2^m$, and $\mathbb{C}^n = \left(\mathbb{C}^2\right)^{\otimes m}$. Haar uniformity is attained by choosing the c_{ij} independently from a Gaussian distribution with vanishing mean and finite variance [22, 31–33]. The obtained state in each run will have to be normalized to unity.

The probability density function for the Gaussian distribution is given by

$$f_{\mathrm{G}}(x) = \frac{1}{\sigma_{\mathrm{G}}\sqrt{2\pi}} \mathrm{e}^{-\frac{1}{2}\left(\frac{x-\mu_{\mathrm{G}}}{\sigma_{\mathrm{G}}}\right)^2}, \tag{2}$$

where μ_{G} is the mean and σ_{G} is the standard deviation of the distribution. The corresponding semi-interquartile range, which is half of the difference between the third and first quartiles of the distribution function, is given by

$$\gamma_{\mathrm{G}} \approx 0.67448 \times \sigma_{\mathrm{G}}. \tag{3}$$

The un-normalized random states are distributed in a hyperspace of dimension n, when the real numbers are chosen from the Gaussian distribution with zero mean and unit variance. Once the states are normalized, they are distributed uniformly over a hypersphere of unit radius in that space. As an illustration, let us consider the space of three orthonormal vectors with *real* coefficients,

$$|\phi\rangle = \sum_{i=1}^{3} c_i|i\rangle. \tag{4}$$

We can depict this state as the point (c_1, c_2, c_3) in $\mathbb{R}^3$. In figure 1(a), we plot a scatter diagram of these points for a large number of realizations of the un-normalized state, $|\phi\rangle$. It may be noted that the joint probability distribution of three independent variables, x, y, z, is spherically symmetric, if the individual distributions are Gaussian. For example, with mean $\mu_{\mathrm{G}} = 0$ and standard deviation $\sigma_{\mathrm{G}} = 1$, the joint probability distribution of x, y, z is

$$f_{\mathrm{G}}(x)f_{\mathrm{G}}(y)f_{\mathrm{G}}(z) = (2\pi)^{-\frac{3}{2}}\, \mathrm{e}^{-\frac{x^2+y^2+z^2}{2}}. \tag{5}$$

The effect of normalization of the state can be seen in figure 2(a). For comparison, we also plot, in the other panels in figures 1 and 2, the un-normalized and normalized states, when c_1, c_2, and c_3 are chosen, independently, from two other distributions separately.

The random numbers utilized to model the disorder, arising in the coefficients of randomly chosen bipartite and tripartite quantum states expressed in the computational basis, have been chosen from Gaussian, uniform, or Cauchy–Lorentz probability distributions.

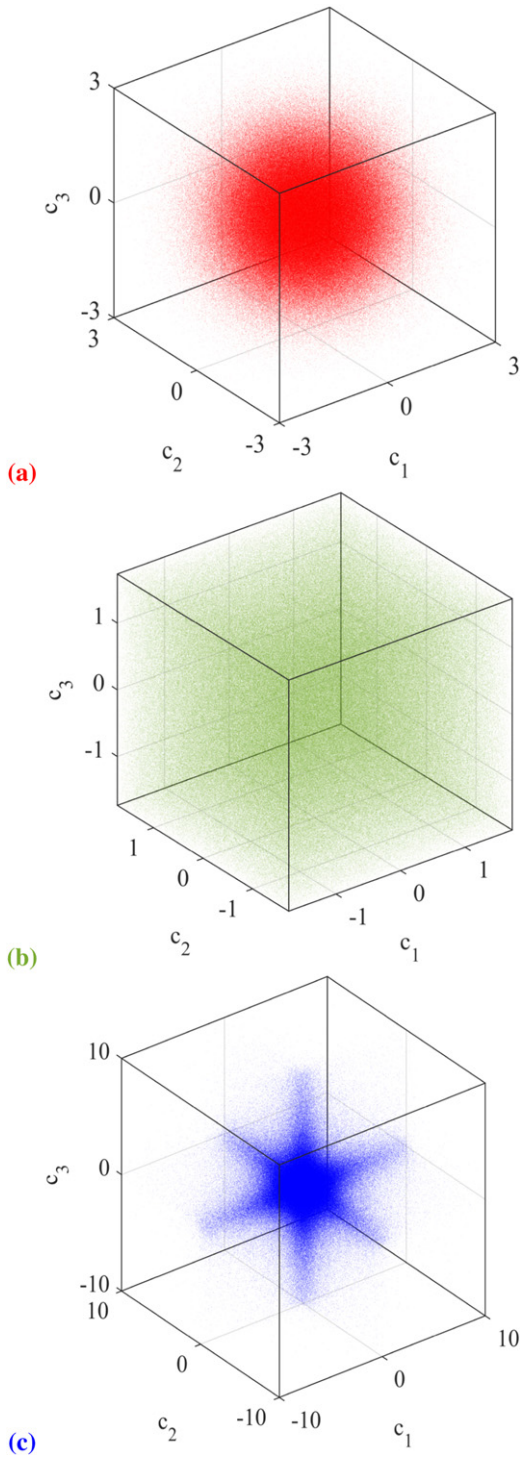

Figure 1. Haar-uniform quantum state generation and comparison with other random generations: un-normalized case. The scatter diagrams in the different panels are generated by independently choosing c_1, c_2, c_3 of equation (4), from different probability distributions. The scatter diagram in panel (a) corresponds to Haar-uniform state generation in a *real* three-dimensional Hilbert space, where the state is not normalized. It is generated by choosing the c_i independently from the Gaussian distribution with mean $\mu_G = 0$ and standard deviation $\sigma_G = 1$. In panel (b), the c_i are independently chosen from the uniform distribution with mean $\mu_U = 0$ and standard deviation $\sigma_U = 1$, so that the range is $-\sqrt{3}$ to $\sqrt{3}$, while in panel (c), we use the Cauchy–Lorentz distribution of median $x_0 = 0$ and semi-interquartile range $\gamma_{C-L} \approx 0.67\,448$. Note that the Gaussian distribution with standard deviation $\sigma_G = 1$ has a semi-interquartile range of $\gamma_G \approx 0.67\,448$. Note also that the states generated in panels (b) and (c) are *not* Haar-uniform. All quantities plotted are dimensionless.

The probability density function for the uniform distribution is

$$f_U(x) = \begin{cases} \dfrac{1}{b-a}, & \text{if } a \leqslant x \leqslant b, \\ 0, & \text{otherwise.} \end{cases} \tag{6}$$

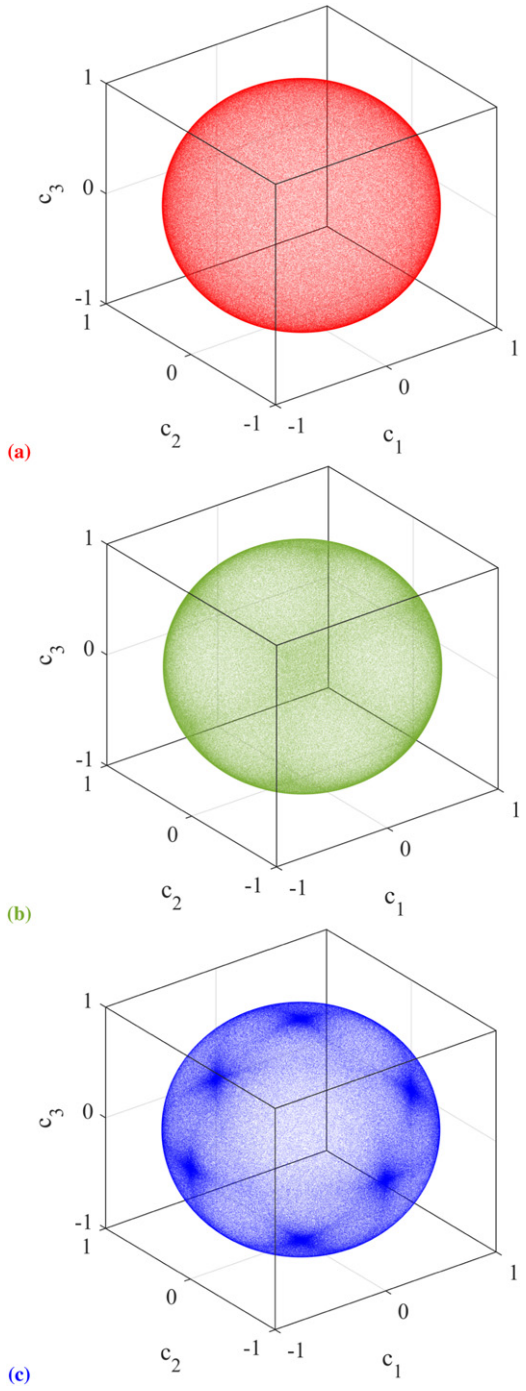

Figure 2. Haar-uniform quantum state generation and comparison with other random generations: normalized case. The considerations in the scatter diagrams here are exactly the same as in the respective panels in figure 2, except that the quantum states are normalized to unity here.

The mean, standard deviation and semi-interquartile range in this case are given respectively by

$$\mu_{\mathrm{U}} = \frac{b+a}{2}, \qquad \sigma_{\mathrm{U}} = \frac{b-a}{2\sqrt{3}} \quad \text{and} \quad \gamma_{\mathrm{U}} = \frac{b-a}{4}. \tag{7}$$

The probability density function of the uniform distribution in terms of its mean and standard deviation can be written as

$$f_{\mathrm{U}}(x) = \begin{cases} \dfrac{1}{2\sqrt{3}\sigma_{\mathrm{U}}}, & \text{if } \mu_{\mathrm{U}} - \sqrt{3}\sigma_{\mathrm{U}} \leqslant x \leqslant \mu_{\mathrm{U}} + \sqrt{3}\sigma_{\mathrm{U}}, \\ 0, & \text{otherwise.} \end{cases} \tag{8}$$

The Cauchy–Lorentz probability density function is given by

$$f_{\mathrm{C-L}}(x|x_0,\gamma_{\mathrm{C-L}}) = \frac{\gamma_{\mathrm{C-L}}}{\pi\left[\gamma_{\mathrm{C-L}}^2 + (x-x_0)^2\right]}, \tag{9}$$

where x_0 is the median of the distribution and $\gamma_{\mathrm{C-L}}$ is the scale parameter, being equal to its half width at half maximum or semi-interquartile range. The mean and variance of the Cauchy–Lorentz distribution are not well-defined. The Cauchy principal value of the mean does exist, and equals the median. In absence of the mean, we use the median as a measure of central tendency of the distribution. And in absence of the standard deviation, we use the semi-interquartile range as a measure of dispersion of the distribution. The corresponding cumulative distribution function is

$$F_{\mathrm{C-L}}(x|x_0,\gamma_{\mathrm{C-L}}) = \int_{-\infty}^{x} f_{\mathrm{C-L}}(x'|x_0,\gamma_{\mathrm{C-L}})\mathrm{d}x' = \frac{1}{\pi}\tan^{-1}\left(\frac{x-x_0}{\gamma_{\mathrm{C-L}}}\right) + \frac{1}{2}. \tag{10}$$

Therefore, the quantile function or the inverse cumulative distribution function is

$$x = x_0 + \gamma_{\mathrm{C-L}}\ \tan\left[\pi\left(F_{\mathrm{C-L}} - \frac{1}{2}\right)\right]. \tag{11}$$

This quantile function generates a random number from the Cauchy–Lorentz distribution when $F_{\mathrm{C-L}}$ is randomly chosen from a uniform distribution in the range 0 to 1.

2.2. Entanglement measures

We wish to analyze entanglement in bipartite and tripartite quantum states. The bipartite quantum states that we will encounter are all two-qubit states, and therefore, we can use the concurrence to measure their entanglement contents. Concurrence of a two-qubit density matrix ρ is defined as

$$C(\rho) = \max\{0, \lambda_1 - \lambda_2 - \lambda_3 - \lambda_4\}, \tag{12}$$

where the λ_i's are square roots of the eigenvalues of $\rho\tilde{\rho}$ in descending order. Here $\tilde{\rho}$ is the spin-flipped ρ: $\tilde{\rho} = (\sigma_y \otimes \sigma_y)\rho^*(\sigma_y \otimes \sigma_y)$, ρ^* is the complex conjugate of ρ in the computational basis [28, 29]. The physical meaning of the concurrence is obtained through its relation, for two-qubit states, with the entanglement of formation [34, 35]. And the entanglement of formation of a bipartite state, not necessarily of two qubits, is a quantifier of the 'amount' of singlets necessary to create the state by LOCC.

We now move over to the tripartite case, where we use a computable multiparty entanglement monotone, for both pure and mixed states, given in reference [30]. The measure is equal to the negativity [36–41] for the bipartite case, and can be considered to be an extension of negativity to the multipartite case. A tripartite state ρ_{ABC} is not biseparable (i.e. not a convex combination of states which are separable in at least one bipartition) and therefore genuinely multiparty entangled if

$$\rho_{\mathrm{ABC}} \neq p_1\rho_{\mathrm{A|BC}}^{\mathrm{sep}} + p_2\rho_{\mathrm{B|CA}}^{\mathrm{sep}} + p_3\rho_{\mathrm{C|AB}}^{\mathrm{sep}}, \tag{13}$$

where $\rho_{\mathrm{A|BC}}^{\mathrm{sep}} = \sum_k q_k|\phi_{\mathrm{A}}^k\rangle\langle\phi_{\mathrm{A}}^k| \otimes |\psi_{\mathrm{BC}}^k\rangle\langle\psi_{\mathrm{BC}}^k|$, etc., and $\{p_i\}$, $\{q_k\}$ are probability distributions. Since any biseparable state is a PPT mixture (i.e. is a convex combination of states that are non-negative under partial transpose (PPT) in at least one bipartition), a state which is not a PPT mixture is necessarily genuine multipartite entangled [36, 37]. Therefore, the state ρ_{ABC} is genuinely multiparty entangled if

$$\rho_{\mathrm{ABC}} \neq p_1\rho_{\mathrm{A|BC}}^{\mathrm{PPT}} + p_2\rho_{\mathrm{B|CA}}^{\mathrm{PPT}} + p_3\rho_{\mathrm{C|AB}}^{\mathrm{PPT}}, \tag{14}$$

where $\rho_{\mathrm{A|BC}}^{\mathrm{PPT}}$, etc. are states which have a non-negative partial transpose with respect to the indicated bipartition. The genuine entanglement content of this state is characterized and quantified by an entanglement witness W, which is an observable that is non-negative on all biseparable states but has a negative expectation value on at least one entangled state [42]. A witness W is fully decomposable if, for every subset M of a system, it is decomposable with respect to the bipartition given by M and its complement $\overline{M}$, which implies that there exist positive semidefinite operators P_M and Q_M such that

$$\text{for all } M : W = P_M + Q_M^{T_M}, \tag{15}$$

where T_M is the partial transpose with respect to M. This observable is non-negative on all PPT mixtures, as it is so on all states which are PPT with respect to some bipartition.

Given a multipartite state ρ, if

$$\min\ \mathrm{Tr}(W\rho) \tag{16}$$

is negative, then ρ is not a PPT mixture, so that it is genuinely multipartite entangled. The negative of the witness expectation value, with the conditions $0 \leqslant P_M \leqslant 1$ and $0 \leqslant Q_M \leqslant 1$, is defined as the measure of genuine multipartite entanglement. It satisfies the properties of a good entanglement measure [30].

The MATLAB code for this multipartite entanglement measure which require semi-definite programming [43] has been provided by Jungnitsch at [44], and has been used in the calculation of the measure in this work.

2.3. Disorder and averaging

Disorder can appear in different hues and patterns in a physical system. We consider here a type of disorder that has often been referred to in the literature as 'quenched' [45–50]. This is to be differentiated from the quenching in the dynamics of a physical system. Within this type of disorder, which is also called 'glassy', the equilibration of the disorder in the system takes a time that is several orders of magnitude higher than the time required to observe the system characteristics which are relevant to our purposes. The system's physical characteristics, as understood from the values of its physical quantities under consideration, have to be averaged over the disorder to obtain physically meaningful numbers. However, because of the nature of disorder chosen, the averaging needs to be performed only after all physical quantities for given realizations of the disorder have been already calculated. This mode of averaging has sometimes been referred to in the literature as 'quenched averaging' [51–53]. We will however refer to the disorder considered and its averaging without any adjectives.

2.4. Third and fourth moments

For a data set with data points $\{(x_1, y_1), (x_2, y_2), \ldots, (x_N, y_N)\}$ the skewness and kurtosis are defined as follows:

$$s = \frac{\sum_{i=1}^{N} (y_i - \mu)^3}{N\sigma^3}, \tag{17}$$

$$k = \frac{\sum_{i=1}^{N} (y_i - \mu)^4}{N\sigma^4}, \tag{18}$$

where μ and σ are the mean and the standard deviation of the corresponding data set. Skewness is a measure of asymmetry of the distribution. It is negative when the distribution is left skewed or has a longer left tail and positive for a right skewed distribution or a distribution with a longer right tail [54]. Kurtosis is a measure which determines the tendency of the distribution to produce outliers [55]. Note that up to the scaling by a power of the standard deviation, the skewness and kurtosis are respectively the third and fourth central moments.

3. Response of bipartite and tripartite entanglement to disorder

An arbitrary two-qubit pure state is given by

$$|\psi\rangle = (\alpha_1 + \mathrm{i}\alpha_2)\,|00\rangle + (\beta_1 + \mathrm{i}\beta_2)\,|01\rangle + (\gamma_1 + \mathrm{i}\gamma_2)\,|10\rangle + (\delta_1 + \mathrm{i}\delta_2)\,|11\rangle\,, \tag{19}$$

where α_1, α_2, β_1, β_2, γ_1, γ_2, δ_1, δ_2 are real numbers, constrained by the normalization condition, $\langle\psi|\psi\rangle = 1$. The state in Equation (19) can be Haar-uniformly generated by randomly choosing the eight real coefficients independently from a normal (Gaussian) distribution of mean $\mu_{\mathrm{G}} = 0$ and a finite standard deviation, followed by a normalization [22, 33, 56–60]. Here we choose the random numbers independently from the standard normal distribution, i.e. the Gaussian distribution with mean $\mu_{\mathrm{G}} = 0$ and standard deviation $\sigma_{\mathrm{G}} = 1$.

'First step'. A large number (10^7) of such random pure states are generated and the concurrence of each state is calculated. Thus, an entanglement distribution for random two-qubit pure states is obtained, with the range being from 0 till 1. The relative frequency percentages of the distribution for different concurrences is plotted as black asterisks in figure 3.

'Second step'. Next, we introduce disorder at α_1 using Gaussian, uniform, or Cauchy–Lorentz distribution functions. We begin with the Gaussian case. One hundred random pure states are generated by choosing random numbers from the Gaussian distribution with $\mu_{\mathrm{G}} = \alpha_1$, where α_1 is the random number generated in the first step, and $\gamma_{\mathrm{G}} = 1/2$, which corresponds to $\sigma_{\mathrm{G}} \approx 0.74131$. The value of σ_{G} here should not be confused with the value of σ_{G} in the context of Haar uniformity. The value of σ_{G} here refers to the scope of error in the chosen coefficient only. These random numbers are the new α_1s (in the disordered case), while the other random numbers are the ones selected in the first step, prior to normalization. The random pure states are normalized and their average entanglement calculated. This therefore provides us with another set

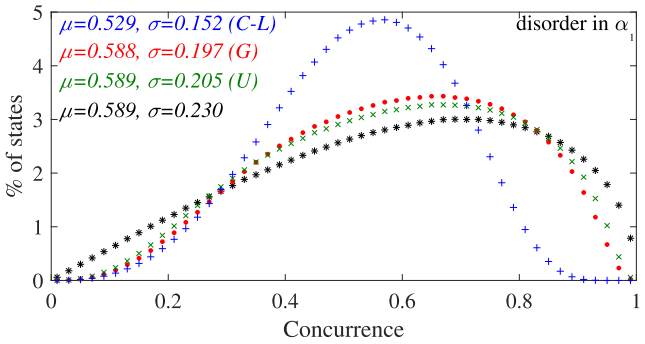

Figure 3. Inhibition of spread of two-party pure quantum state entanglement in response to disorder. We plot here the percentages (precisely, relative frequency percentages) of Haar-uniformly chosen two-qubit pure states $|\psi\rangle$, given by equation (19), with and without disorder at α_1, against the concurrence values, with the latter ranging between 0 and 1. The black asterisks correspond to percentages of random two-qubit pure states generated Haar uniformly, while the other three curves depict entanglement distributions for random two-qubit pure states with disorder at α_1 chosen from Gaussian (G, red dots), uniform (U, green crosses), and Cauchy–Lorentz (C–L, blue pluses) distributions. The disorder averaged values plotted in the figure are for 100 disorder configurations for every α_1. The figure does not change up to the precision used for averaging over 50 configurations. The initial Haar-uniform generation (in the 'first step') used for the figure utilizes 10^7 states (and hence the same number of α_1s), although the same plot does not alter, up to the precision used, for 10^6 points. The precision is checked to three significant figures. The calculation of the relative frequency percentages requires a window on the horizontal axis, and it is 0.02 ebits. The convergence checking is done for all other later figures also, but is not explicitly repeated there. The numbers corresponding to the Haar-uniform generation and disorder generation remain the same throughout except the last two figures depicting three qubit entanglement. The precision and the horizontal axis window are also the same in all figures, except the last two, which relate to three-qubit systems. The vertical axis is dimensionless, while the horizontal one is in ebits, which again is the same in all figures except the last two. The skewness and kurtosis of the plot in the ordered case are respectively $s = -0.292$ and $k = 2.20$, while for the disordered cases, they are $s(\mathrm{U}) = -0.214$, $k(\mathrm{U}) = 2.17$; $s(\mathrm{G}) = -0.219$, $k(\mathrm{G}) = 2.22$; $s(\mathrm{C–L}) = -0.253$, $k(\mathrm{C–L}) = 2.56$, respectively for disorders from uniform, Gaussian, and Cauchy–Lorentz distributions.

of 10^7 disorder averaged entanglement values, and again for this distribution, we plot the corresponding relative frequency percentages for different concurrences, as red dots in figure 3.

The average entanglement for the Haar-uniformly chosen random pure two qubit states is 0.589, while the corresponding standard deviation is 0.230. This is the clean case, i.e. the case without disorder. It can be seen from figure 3 that introduction of disorder in the parameter α_1 from Gaussian distribution does not affect the average entanglement (equaling 0.588). However, the standard deviation of the corresponding entanglement distribution is reduced (being 0.197).

We therefore find that the distribution of entanglement of Haar-uniformly chosen quantum states is not uniform in the entire range of possible values, viz $[0, 1]$, but is concentrated at an intermediate point in $[0, 1]$. Moreover, *introduction of disorder in the parameters of the Haar-uniformly generated quantum states leads to a further concentration of values around an intermediate central value*. This of course has been obtained in a case that is highly specific from several perspectives. *The question that we ask is whether this feature is generic*. To answer this question, we try to remove the specificity of the case studied, viz checking the response in pure two-party quantum entanglement to Gaussian disorder in a single parameter, from several perspectives.

The Haar-uniform generation of quantum states spreads out the states in the most uniform pattern on the state space. Any variation of that by putting in noise or disorder will make it less uniform. However, this does not necessarily mean that the less uniform distribution has lower standard deviation, as the lower uniformity can result in clustering at different places in the state space. As an example, let us consider 101 points uniformly distributed over the range $[0, 1]$. This distribution has a standard deviation of approximately 0.29. However, if the same points are non-uniformly distributed with 51 at 0 and 50 at 1, the standard deviation will be approximately 0.50. Moreover, we calculate the standard deviations of the distributions of entanglement of the states obtained from a given distribution with or without disorder insertion. Entanglement is a nonlinear function of the state parameters, which makes it even more nontrivial to easily infer the dispersion at the level of entanglement from that at the level of state parameters.

Before investigating the effects of disorders randomly drawn from non-Gaussian distributions, we will explore the reason behind the apparent non-intuitive effect of disorder on random quantum states, viz, the inhibition of the spread of entanglement in response to disorder. We focus on Haar uniformly chosen states with values of concurrence, measured in ebits, in the range $(C_i - \Delta, C_i + \Delta)$, separately for $C_i = 0.1, 0.2, \ldots, 0.9$, and for $\Delta = 0.01$. These quantum states are perturbed at a single parameter (α_1 of equation (19)) using disorder chosen from Gaussian distributions with $\mu_{\mathrm{G}} = \alpha_1$, and $\gamma_{\mathrm{G}} = 1/2$. Figure 4 shows the response of this Gaussian disorder in a single parameter on the distribution of concurrence. It

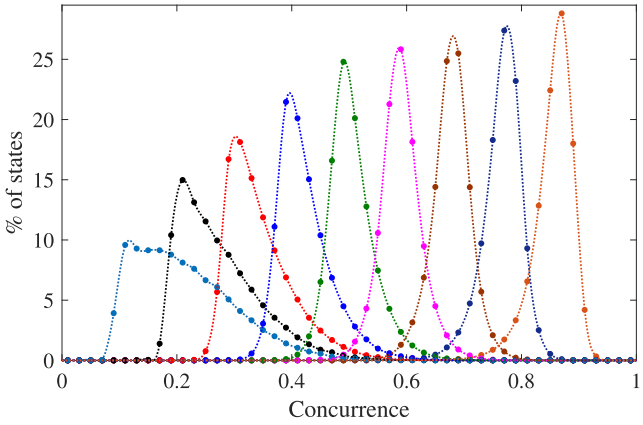

Figure 4. Spread of two-party pure quantum state entanglement in response to disorder in a single parameter. We plot here the relative frequency percentages of Haar-uniformly chosen two-qubit pure states $|\psi\rangle$, given by equation (19), with concurrence values in ebits in the ranges 0.1 ± 0.01 (cyan dots), 0.2 ± 0.01 (black dots), 0.3 ± 0.01 (red dots), 0.4 ± 0.01 (blue dots), 0.5 ± 0.01 (green dots), 0.6 ± 0.01 (magenta dots), 0.7 ± 0.01 (brown dots), 0.8 ± 0.01 (deep blue dots), 0.9 ± 0.01 (orange dots), with disorder at α_1 chosen from Gaussian distributions. These quantities, for the different cases are on the vertical axis, and are plotted against the concurrence values, with the latter ranging between 0 and 1, clustered in small sub-ranges. The disorder averaged values plotted in the figure are for 100 disorder configurations. The figure does not change, up to the precision used, for averaging over 50 configurations. The precision is checked to two significant figures. The vertical axis is dimensionless, while the horizontal one is in ebits. The skewnesses of the plots are 0.81, 1.1, 1.2, 1.1, 0.86, 0.34, −0.26, -0.83, −1.3, respectively for the plots from left to right. Please see text for more details.

Table 1. Comparison of concurrences before and after the introduction of disorder at one parameter. The single parameter in which disorder is introduced is α_1 of equation (19). The first row denotes the midpoint of the range $(C_i - \Delta, C_i + \Delta)$. The second row denotes the average of the concurrences of the disorder-induced distribution of states for that range. See text for more details.

C_i	0.1	0.2	0.3	0.4	0.5	0.6	0.7	0.8	0.9
Average	0.21	0.27	0.34	0.42	0.51	0.59	0.68	0.77	0.86

can be seen that the distributions are positively skewed for the entanglement, $C_i = 0.1, 0.2, \ldots, 0.6$ and negatively skewed for 0.7, 0.8, and 0.9. Note that the average value of entanglement, as obtained from these distributions, and exhibited in table 1 varies accordingly. Therefore, it seems that as we perturb a quantum state which has a certain value of concurrence, it has greater probability to transform into a state with higher or lower entanglement depending on whether the parent state had a value of entanglement that was lower or higher than the average entanglement of Haar uniformly distributed states in the ordered case. The value of the latter is 0.589 ebits. As an example, we may refer to the curve with black dots in figure 4, which corresponds to $C_i = 0.2$ ebits, which is therefore less than 0.589. After the insertion of disorder, the average of the distribution corresponding to $C_i = 0.2$ moves toward 0.589. The opposite happens for $C_i = 0.8$. We will find that this skewed effect of disorder is similar, although more pronounced, when disorder is applied in four parameters of the Haar uniformly chosen random quantum states.

3.1. Non-Gaussian disorder

For investigating the question of genericity, the first of the removals of specificity is effected by considering non-Gaussian disorder distributions. Therefore, the 'second step' mentioned above is followed to separately introduce disorder at α_1 from the uniform and Cauchy–Lorentz distributions, instead of the Gaussian one. For the case of the uniform distribution, random numbers are selected from a uniform distribution with $\mu_{\rm U} = \alpha_1$, where α_1 is the random number generated in the first step, and $\gamma_{\rm U} = 1/2$. In the Cauchy–Lorentz case, disorder is introduced at α_1 by choosing random numbers from a Cauchy–Lorentz distribution with median $x_0 = \alpha_1$ and semi-interquartile range $\gamma_{\rm C-L} = 1/2$. Note that the mean is equal to the median for the Gaussian and uniform distributions. The data for the uniform distribution is plotted as green crosses, and that for the Cauchy–Lorentz as blue pluses, in figure 3.

As already reported above, the average entanglement for the Haar-uniformly chosen random pure two qubit states is 0.589, while the corresponding standard deviation is 0.230, in the ordered (clean) case. All numbers in the calculations for the two-qubit cases are correct to three significant figures. The equality symbols used in the corresponding figures are up to this precision. It can be seen from figure 3 that introduction of disorder in the parameter α_1 from Gaussian and uniform distributions does not affect the disorder averaged entanglement (equaling 0.588 in the former case, as already reported above, and 0.589 in

the latter one). However, the disorder averaged standard deviations of the corresponding entanglement distributions are reduced (being 0.197 in the case of Gaussian disorder, as already reported above, and 0.205 in the uniform case). There are appreciable changes in both mean and standard deviation (being respectively 0.529 and 0.152) of the entanglement distribution when the disorder in the parameter α_1 is from the Cauchy–Lorentz distribution.

The mean and the standard deviation provide important information about the relative frequency distribution of random states as a function of concurrence. The mean and standard deviation are respectively the first raw moment and the second central moment of a distribution. There are of course higher moments that can be analyzed to gather further information about the distribution under consideration. To investigate the distribution further we employ two higher order central moments scaled by the standard deviation, viz skewness (s) and kurtosis (k). We find that the plots in the ordered cases are left skewed, and after inclusion of disorder, the left-skewness decreases slightly in all the three cases of disorder considered. The kurtosis for the clean case is almost identical with the cases when disorders are introduced from the Gaussian and uniform distributions, while the kurtosis increases when the disorder is introduced from the Cauchy–Lorentz distribution, indicating an increase of outliers. The values of skewness and kurtosis for the frequency distributions are mentioned in the caption of figure 3.

So we find that altering the distribution of disorder does not alter the fact that the disorder results in an inhibition of spread of the entanglement distribution. In fact, moving over to the Cauchy–Lorentz case makes the inhibition significantly more pronounced.

3.2. Noisy two-qubit states

For two-party pure states, the local von Neumann entropy is a 'good' measure of entanglement [34]. And for two-qubit pure states, this is equivalent to the concurrence [28, 29]. We however use concurrence to measure entanglement of two-qubit pure states, to be able to consider the response of disorder on entanglement of two-qubit pure states admixed with noise, thus leading to mixed states, for which, von Neumann entropy of local density matrices does not quantify entanglement, while concurrence does.

The intention in this subsection is to look at the effect, on the response to disorder that we have already seen above, of noise admixture in the states involved. More precisely, we consider a Haar-uniformly generated set of states, $|\psi\rangle$, given by equation (19), with each admixed with white noise, so that the actual state is

$$\varrho = p|\psi\rangle\langle\psi| + (1-p)\frac{1}{4}I_4. \tag{20}$$

We consider a fixed p for every $|\psi\rangle$, so that we can assume that we are dealing with a situation where any of the randomly generated states are passing through a fixed noisy channel, that admixes the input with white noise with a fixed noise level. The state ϱ of course depends on the state $|\psi\rangle$ and the noise parameter p, which are kept silent in the notation. Here, I_4 represents the identity operator on the two-qubit Hilbert space.

We fix attention on the Cauchy–Lorentz disorder distribution, and compare the corresponding disorder averaged entanglement spread in the noisy states with that in the noisy case without disorder. We find that the feature of inhibition of spread remains valid even in this noisy situation. The results are plotted in figure 5, where two different values of the noise level, viz $p = 0.9$ and $p = 0.8$, are considered. Both the mean and standard deviation are affected by the disorder, and in particular for $p = 0.9$, the disorder averaged standard deviation is 0.159, while the standard deviation in the clean case is 0.207. A similar inhibition of the spread is observed for $p = 0.8$, as exhibited in the same figure.

Two points could be mentioned before we move away from this noisy case. Firstly, note that noise itself also leads to an inhibition of the spread.

Secondly, the curves of the percentages of states, when plotted against entanglement (as quantified by concurrence) are non-monotonic. However, in the noiseless cases, all of them have a bell-like shape, and in particular do not have any non-monotonicity near zero entanglement. In the noisy case, there appears an additional non-monotonicity near zero entanglement (in the clean cases). This is not due to any numerical convergence problem, and, e.g. the percentage of zero entanglement states in the clean case for $p = 0.8$ is 2.32%, which remains the same irrespective of whether 10^7 or 10^6 states are considered in the Haar-uniform generation, up to three significant figures. This additional non-monotonicity near zero entanglement can be expected from the fact that the noise inflicted has brought the original set of states closer to the separable ball, and has resulted in more states clustered near the zero-entanglement point. We will come back to this point again when we consider noisy three-qubit states below, where this additional non-monotonicity will be absent. Note that the percentage of zero entanglement states decreases with increasing p, as expected. We remember that increasing p corresponds to decrease in noise. Note also that this additional

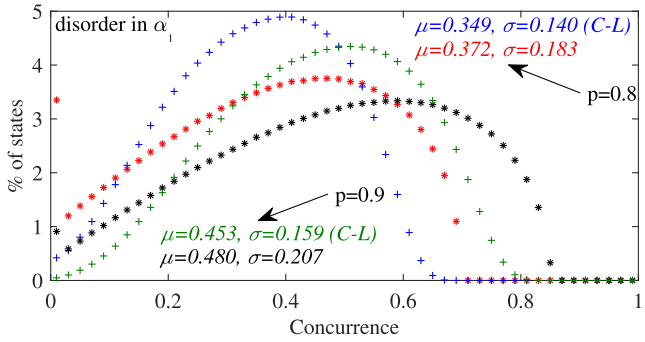

Figure 5. Effect of noise on the inhibited spread of two-party entanglement due to disorder insertion. The considerations in this figure are the same as in the preceding one, except that only the Cauchy–Lorentz disorder is considered, and that the states are admixed with white noise. The symbols are also different in this figure as compared to the preceding one. The black asterisks and the green pluses depict the case when noise-level is given by $p = 0.9$, with the asterisks being for the clean case and the pluses for the disorder averaged situation. The red asterisks and the blue pluses are similarly for $p = 0.8$. For $p = 0.9$ the skewness and kurtosis for the clean case are $s(p = 0.9) = -0.288$ and $k(p = 0.9) = 2.19$, while for the disordered case the corresponding values are $s(\text{C–L}; p = 0.9) = -0.229$ and $k(\text{C–L}; p = 0.9) = 2.30$. Similarly for $p = 0.8$ the skewness and kurtosis for the clean case are $s(p = 0.8) = -0.253$ and $k(p = 0.8) = 2.11$, while for the disordered case the corresponding values are $s(\text{C–L}; p = 0.8) = -0.201$ and $k(\text{C–L}; p = 0.8) = 2.25$. Note that the 'disordered distributions' have marginally lesser left-skewness and marginally higher kurtosis. For a discussion on the additional non-monotonicity near zero entanglement that occurs in this noisy case for the curves corresponding to the clean situations, see text.

non-monotonicity does not remain in the disordered case, due to the smearing-out effect of the disorder averaging process.

3.3. Disorder in multiple parameters

We revert to pure states, but now consider disorder in multiple parameters. Note that in the considerations until now, we have analyzed situations where there is disorder only in one parameter of the Haar-uniformly generated state, $|\psi\rangle$, in equation (19).

3.3.1. Two parameters

We now analyze the situation where disorder is introduced in *two* parameters, viz α_1 and β_1, independently from Gaussian, uniform, or Cauchy–Lorentz distributions. Random numbers are selected from Gaussian, uniform distributions with $\mu_{\text{G/U}} = \alpha_1$, $\gamma_{\text{G/U}} = 1/2$ and $\mu_{\text{G/U}} = \beta_1$, $\gamma_{\text{G/U}} = 1/2$, while random numbers are chosen from Cauchy–Lorentz distributions with $x_0 = \alpha_1$, $\gamma_{\text{C–L}} = 1/2$ and $x_0 = \beta_1$, $\gamma_{\text{C–L}} = 1/2$. These random numbers are the new α_1s and β_1s in equation (19), while the other random numbers are the ones selected in the first step, prior to normalization. One hundred such pure states are generated and the average entanglement with disorder is calculated. The resulting entanglement distributions are plotted in figure 6. It can be seen from figure 6 that introduction of disorder in both the parameters α_1 and β_1 from Gaussian and uniform distributions does not affect the average entanglement appreciably (being 0.586 in the Gaussian case and 0.588 in the uniform one). However, the standard deviations of the corresponding entanglement distributions are reduced further (being 0.170 in the Gaussian case and 0.184 in the uniform one) in comparison with the matching cases where disorder was introduced in the coefficient α_1 only. There are appreciable changes in both mean and standard deviation (being respectively 0.528 and 0.138) of the entanglement distributions when the disorders in the parameters α_1 and β_1 are randomly chosen from the Cauchy–Lorentz distribution, and again the standard deviation is lower than when a Cauchy–Lorentz disorder was inserted only in the parameter α_1 (compare with figure 3).

3.3.2. Four parameters

We have already seen that introducing disorder in two parameters leads to increased restriction, in comparison to when we introduce the same in one parameter, on the spread of entanglement on the span $[0, 1]$. Does this increase in restriction to spread continue when we introduce disorder in even further parameters? In an attempt to find this answer, we now consider the effect of introducing disorder in four parameters.

Therefore, we now introduce disorder in the parameters α_1, β_1, γ_1, and δ_1 independently from Gaussian, uniform, or Cauchy–Lorentz distributions. Random numbers for introduction of disorder are selected from Gaussian or uniform distributions with

$$\mu_{\text{G/U}} = \alpha_1, \quad \gamma_{\text{G/U}} = 1/2, \quad \mu_{\text{G/U}} = \beta_1, \quad \gamma_{\text{G/U}} = 1/2,$$
$$\mu_{\text{G/U}} = \gamma_1, \quad \gamma_{\text{G/U}} = 1/2, \quad \mu_{\text{G/U}} = \delta_1, \quad \gamma_{\text{G/U}} = 1/2,$$

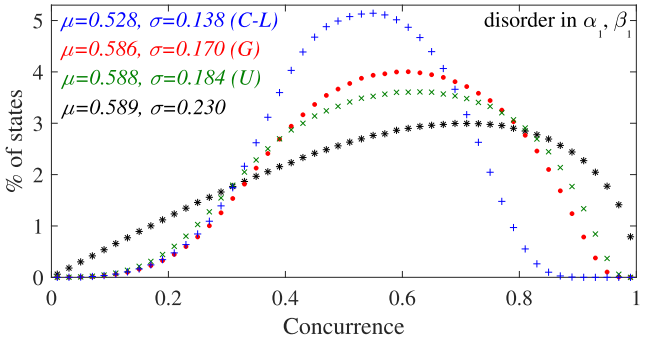

Figure 6. Further hindrance to entanglement spread as we introduce disorder in more parameters. The case of introducing disorder in two parameters is considered in this figure, while the case of doing the same for four parameters is considered in the succeeding figure. The considerations are the same as in figure 3, except that the disorder is introduced in α_1 and β_1, instead of just α_1. The skewness and kurtosis of the ordered plot are $s = -0.292$ and $k = 2.20$, while for the plots in the disordered cases, the skewness and kurtosis are $s(\mathrm{U}) = -0.159$, $k(\mathrm{U}) = 2.27$; $s(\mathrm{G}) = -0.171$, $k(\mathrm{G}) = 2.33$; $s(\mathrm{C–L}) = -0.209$, $k(\mathrm{C–L}) = 2.56$, for disorders from uniform, Gaussian, and Cauchy–Lorentz distributions respectively. The disordered plots are less left skewed in comparison with the clean case, the left skewness of the disordered plots have also decreased in comparison with the cases when disorder was introduced in one parameter. The kurtosis is seen to increase slightly for the disordered cases.

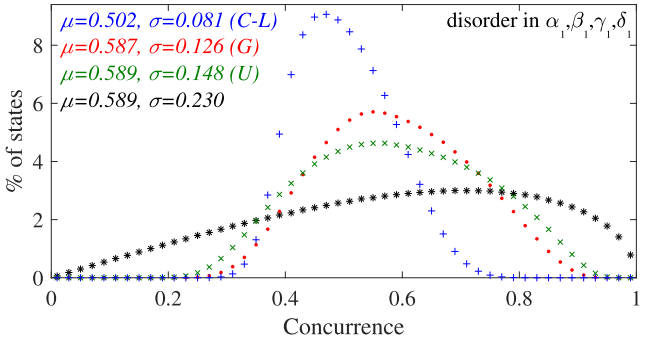

Figure 7. Disorder in four parameters lead to increased restriction, in comparison to the case when disorder was introduced in two parameters, in spread of entanglement in two-qubit states. All considerations except the increased number of parameters is the same as in the preceding figure. The skewness and kurtosis of the ordered plot are $s = -0.292$ and $k = 2.20$ as mentioned in figure captions before. For the disordered case, the skewness and kurtosis are $s(\mathrm{U}) = 0.0406$, $k(\mathrm{U}) = 2.22$; $s(\mathrm{G}) = 0.0976$, $k(\mathrm{G}) = 2.36$; $s(\mathrm{C–L}) = 0.314$, $k(\mathrm{C–L}) = 2.58$, for disorders from uniform, Gaussian and Cauchy–Lorentz distributions respectively. The disordered distributions are now right skewed while the increase of kurtosis is only marginal.

while random numbers are chosen from Cauchy–Lorentz distributions with

$$x_0 = \alpha_1, \quad \gamma_{\mathrm{C–L}} = 1/2, \quad x_0 = \beta_1, \quad \gamma_{\mathrm{C–L}} = 1/2,$$
$$x_0 = \gamma_1, \quad \gamma_{\mathrm{C–L}} = 1/2, \quad x_0 = \delta_1, \quad \gamma_{\mathrm{C–L}} = 1/2.$$

These random numbers are the new α_1s, β_1s, γ_1s, and δ_1s, while the other random numbers are the ones selected in the first step, prior to normalization. Once more, one hundred such pure states are generated and the disorder averaged entanglement is calculated. The resulting entanglement distributions are plotted in figure 7. It can be seen from figure 7 that introduction of disorder in the four parameters α_1, β_1, γ_1, and δ_1 from Gaussian or uniform distributions again does not appreciably affect the average entanglement (being 0.587 in the Gaussian case and 0.589 in the uniform case) with respect to its value in the clean case. However, the standard deviations of the corresponding entanglement distributions are reduced further than their values in the case when disorder was introduced in two parameters, which themselves were lower than the clean case value. Specifically, the standard deviations are 0.126 and 0.148, respectively for introduction of Gaussian and uniform disorders. There are considerable decreases in both the mean and standard deviation (respectively, 0.502 and 0.081) of the entanglement distributions when the disorder in the parameters α_1, β_1, γ_1, and δ_1 are randomly and independently chosen from the Cauchy–Lorentz distribution.

Let us now revisit our efforts in finding the reason behind the inhibition of the spread of entanglement due to disorder. We had pointed to a possible reason at the beginning of this section, around figure 4 and table 1. We again focus on Haar uniformly chosen states with values of concurrence measured in ebits in the

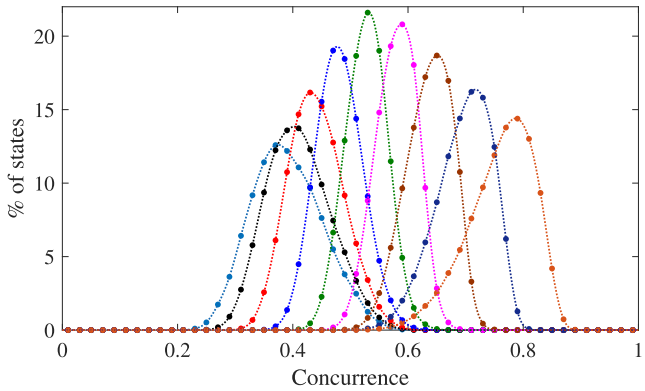

Figure 8. Spread of two-party pure quantum state entanglement in response to disorder in four parameters. The considerations are the same as in figure 4, except that the disorder is introduced in four state parameters. The skewnesses of the plots are 0.23, 0.26, 0.25, 0.17, −0.0029, −0.18, −0.34, −0.51, −0.66, from left to right. See text for more details.

Table 2. Comparison of concurrences before and after the introduction of disorder at four state parameters. The considerations are the same as in table 1, except for the number of parameters in which disorder is introduced.

C_i	0.1	0.2	0.3	0.4	0.5	0.6	0.7	0.8	0.9
Average	0.39	0.41	0.44	0.48	0.53	0.58	0.64	0.70	0.76

ranges 0.1 ± 0.01, 0.2 ± 0.01, ..., 0.9 ± 0.01. These quantum states are perturbed at four parameters α_1, β_1, γ_1, and δ_1 using disorder chosen from Gaussian distributions. Figure 8 depicts the effect of this disorder insertion for the chosen sets of random states. It can be seen that the disordered distributions are positively skewed for $C_i = 0.1, 0.2, 0.3, 0.4$, and negatively skewed for 0.6, 0.7, 0.8, 0.9. The skewness is almost vanishing for 0.5. The curves themselves are significantly right-shifted for states with $C_i = 0.1, 0.2, 0.3, 0.4$ and significantly left-shifted for states with the same equaling 0.8 and 0.9. Note that the average value of entanglement, shown in table 2 varies accordingly. The findings therefore again point to the same realization that as we perturb a quantum state which has a certain value of concurrence, it has greater probability to transform into a state with higher or lower entanglement depending on whether the parent state has an entanglement that is lower or higher than the average entanglement in the ordered case. We moreover find here that the effect of disorder is more pronounced in this case in comparison with the case when disorder is applied in only one parameter of the Haar uniformly chosen random quantum states.

3.4. Effect of variation in dispersion of disorder

We revert to disorder in a single parameter, but stay with pure states. The dispersion, as quantified by the semi-interquartile range, has until now been kept fixed at $1/2$, and which we wish to vary now to see its effect on the inhibition of spread of entanglement. Changing the semi-interquartile range can be interpreted as varying the strength of the disorder introduced, with increase of semi-interquartile range implying increase of the strength. We fix attention on the Gaussian disorder for this purpose, and also introduce the disorder only on a single parameter. Random numbers are selected from Gaussian distributions with $\mu_{\rm G} = \alpha_1$, and $\gamma_{\rm G}$ varying from 0.3 to 0.7 at intervals of 0.1. These random numbers are the new α_1s in equation (19), while the other random numbers are the ones selected in the first step, prior to normalization. Just like in the other cases, one hundred such pure states are generated with the disorder being chosen from the Gaussian distribution, and then the average entanglement is calculated. The resulting entanglement distributions (for different semi-interquartile ranges) are plotted in figure 9. It can be seen from figure 9 that the average entanglement remains almost unchanged with the variation of $\gamma_{\rm G}$, while the standard deviations of the entanglement distributions decrease with the increase of $\gamma_{\rm G}$. Therefore, as the strength of disorder in the states increases, the standard deviations of the resulting entanglement distributions decrease. This feature can help us understand the reason why the Cauchy–Lorentz distribution has consistently been found to lead to greater inhibition of the spread of entanglement in the previous cases, whenever compared with Gaussian and uniform disorder distributions with same semi-interquartile ranges. The Gaussian and uniform distributions have a finite mean, unlike the Cauchy–Lorentz distribution. For two probability distributions (among Gaussian, uniform, and Cauchy–Lorentz) having the same semi-interquartile range, but with one having a finite mean and the other without, we can say that the latter has a longer 'reach' in its domain of definition, viz the real line, that has led to the non-existence of the mean ($\int_{-\infty}^{+\infty} f(x){\rm d}x$ exists and is finite, but $\int_{-\infty}^{+\infty} xf(x){\rm d}x$ does not exist, for a probability density $f(x)$ on the

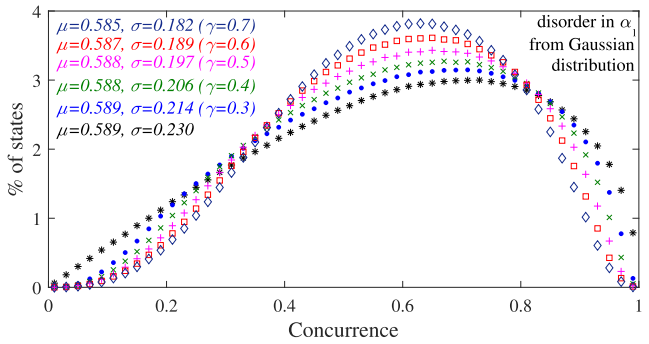

Figure 9. Effect of variation of strength of disorder. The considerations are the same as in figure 3, except that only the Gaussian disorder is considered, and that different semi-interquartile ranges are used for the plots. The symbols are also different here. Black asterisks represent the case when there is no disorder, and has appeared in several figures before, including figure 3. The curve with pink pluses is for $\gamma_G = 1/2$, and was also present in figure 3. The blue (cyan) dots, green crosses, red squares, and blue-black diamonds are respectively for $\gamma_G = 0.3$, 0.4, 0.6, and 0.7. Note that the suffix of γ_G is kept silent in the figure legend on the plot.

real line). And consequently, we can interpret that the latter has a higher dispersion (spread), even though it has the same semi-interquartile range as the former.

3.5. Three-qubit pure states

We now move over to the three-qubit case, considering pure states in this subsection. The succeeding subsection deals with noisy (mixed) three-qubit states. The entanglement measure considered in both this and the succeeding sections is the JMG entanglement monotone. A three-qubit random pure state can be represented as

$$|\Psi\rangle = (a_1 + \mathrm{i}a_2)|000\rangle + (b_1 + \mathrm{i}b_2)|001\rangle + (c_1 + \mathrm{i}c_2)|010\rangle + (d_1 + \mathrm{i}d_2)|011\rangle + (e_1 + \mathrm{i}e_2)|100\rangle + (f_1 + \mathrm{i}f_2)|101\rangle + (g_1 + \mathrm{i}g_2)|110\rangle + (h_1 + \mathrm{i}h_2)|111\rangle. \quad (21)$$

where a_1, a_2, b_1, b_2, c_1, c_2, d_1, d_2, e_1, e_2, f_1, f_2, g_1, g_2, h_1, h_2 are real numbers, constrained by the normalization condition, $\langle\Psi|\Psi\rangle = 1$. The state in equation (21) can be Haar-uniformly generated by randomly choosing the sixteen real coefficients from independent normal distributions of vanishing mean and unit standard deviation, followed by a normalization. A large number (2×10^4) of such random pure states are generated, normalized, and the entanglement monotone of each state is calculated. Next, we introduce disorder at a_1, b_1, c_1, and d_1, independently from Gaussian, uniform, or Cauchy–Lorentz distribution functions. The disorder is introduced by choosing random numbers from Gaussian and uniform distributions with

$$\mu_{G/U} = a_1, \quad \gamma_{G/U} = 1/2, \quad \mu_{G/U} = b_1, \quad \gamma_{G/U} = 1/2,$$
$$\mu_{G/U} = c_1, \quad \gamma_{G/U} = 1/2, \quad \mu_{G/U} = d_1, \quad \gamma_{G/U} = 1/2,$$

where a_1, b_1, c_1, and d_1 are the random numbers generated in the first step. Cauchy–Lorentz distributions with

$$x_0 = a_1, \quad \gamma_{C-L} = 1/2, \quad x_0 = b_1, \quad \gamma_{C-L} = 1/2,$$
$$x_0 = c_1, \quad \gamma_{C-L} = 1/2, \quad x_0 = d_1, \quad \gamma_{C-L} = 1/2,$$

are also used to introduce disorders at a_1, b_1, c_1, and d_1. These random numbers are the new a_1, b_1, c_1, and d_1, while the other random numbers are the ones selected in the first step, prior to normalization. For every set of values of a_1, b_1, c_1, and d_1, chosen in the first step, fifty disordered states are generated by employing the above mentioned procedure. The random pure states are normalized and their average entanglement (the disorder averaged JMG entanglement monotone) calculated. The resulting entanglement distributions are plotted in figure 10. It can be seen from figure 10 that the average entanglement of random three-qubit pure states chosen Haar uniformly is 0.35, while the standard deviation of the entanglement distribution is 0.068. The average entanglement remains constant when disorders are introduced in the coefficients a_1, b_1, c_1, and d_1 from the Gaussian or uniform distributions (being 0.35 for both the cases), while the standard deviations for the entanglement distributions of disordered states are reduced (to 0.052 for the Gaussian case and 0.056 for the uniform one) in comparison to that in the clean case. The average as well as

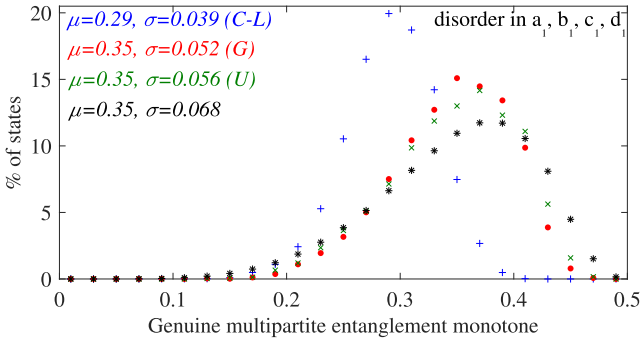

Figure 10. Inhibition of spread of entanglement in the pure three-qubit state space due to insertion of disorder in state parameters. We plot here the relative frequency percentages of Haar-uniformly generated random three-qubit pure states (with and without disorder at a_1, b_1, c_1, d_1) against the JMG entanglement monotone, with the latter ranging between 0 and 1/2. The black asterisks correspond to percentage of random three-qubit pure states generated Haar uniformly, while the other three curves depict entanglement distributions for random three-qubit pure states with disorder at a_1, b_1, c_1, d_1 chosen from Gaussian (G, red dots), uniform (U, green crosses), or Cauchy–Lorentz (C–L, blue pluses) distributions. The numbers in this figure and the succeeding one are correct to two significant figures. The window of the entanglement monotone used for calculating the percentages is 0.02. Both axes represent dimensionless quantities. The skewness and kurtosis of the ordered plot are $s = -0.55$ and $k = 2.9$. For the disordered cases, the skewness and kurtosis are $s(\mathrm{U}) = -0.50$, $k(\mathrm{U}) = 2.9$; $s(\mathrm{G}) = -0.51$, $k(\mathrm{G}) = 3.0$; $s(\mathrm{C–L}) = -0.34$, $k(\mathrm{C–L}) = 3.2$ for disorders from uniform, Gaussian, and Cauchy–Lorentz distributions respectively. The skewness and kurtosis of the frequency distributions, with disorders introduced from the uniform and Gaussian distributions vary slightly with respect to the clean case. The left skewness of the frequency distribution with disorders introduced from the Cauchy–Lorentz distribution, is seen to decrease in comparison with the clean case.

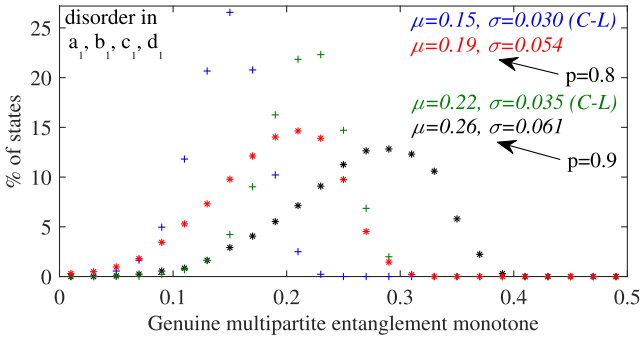

Figure 11. Further disorder-induced inhibition to spread of entanglement of three-qubit states in presence of noise. The considerations are exactly the same as in the preceding figure, except that the states are admixed with white noise, and that only Cauchy–Lorentz disorder is considered. The noise levels considered are given by $p = 0.9$ and $p = 0.8$. For $p = 0.9$, the black asterisks and green pluses represent the clean and disorder-averaged cases respectively. And for $p = 0.8$, the corresponding symbols are respectively red asterisks and blue pluses. For $p = 0.9$, the skewness and kurtosis for the clean case are $s(p = 0.9) = -0.55$ and $k(p = 0.9) = 2.9$, while for the disordered case, the corresponding values are $s(\mathrm{C–L}; p = 0.9) = -0.35$ and $k(\mathrm{C–L}; p = 0.9) = 3.2$ respectively. For $p = 0.8$, the skewness and kurtosis for the clean case are $s(p = 0.8) = -0.50$ and $k(p = 0.8) = 2.9$, while for the disordered case, the corresponding values are $s(\mathrm{C–L}; p = 0.8) = -0.33$ and $k(\mathrm{C–L}; p = 0.8) = 3.2$. The left skewness of the disordered plots decrease in comparison with the clean cases. The kurtosis of the disordered plots increase slightly in comparison with the clean cases, indicating a slightly increased percentage of outliers.

the standard deviation of the entanglement distribution are reduced (to 0.29 and 0.039 respectively) when disorder is introduced in the coefficients a_1, b_1, c_1, and d_1 from the Cauchy–Lorentz distribution.

3.6. Noisy three-qubit states

One could have used simpler measures to quantify genuine multiparty entanglement, if we were required to deal with only pure three-qubit states. An example of such a measure is the generalized geometric measure [61–67]. We have however chosen to work with the JMG entanglement monotone due to its tractability for mixed multiparty states, to be considered in this subsection.

Indeed, in this subsection, we wish to investigate the effect of noise on the restriction of spread of the JMG entanglement monotone in the space of three-qubit states. Precisely, we consider the state

$$\tilde{\varrho} = p|\Psi\rangle\langle\Psi| + (1-p)\frac{1}{8}I_8, \tag{22}$$

for every $|\Psi\rangle$ (see equation (21)) generated in the clean or the disordered cases. Here, I_8 is the identity operator on the three-qubit Hilbert space. This is exactly similar to the analysis in section 3.2, except that

we are considering three-qubit states now, and the measure is the JMG entanglement monotone. The effect obtained is again very similar, viz noise leads to further inhibition of the spread of entanglement. The details of the numerical simulations are presented in figure 11. We have focused attention only on the Cauchy–Lorentz disorder. Just like for the two-qubit case, noise restricts the spread of entanglement even in the clean cases. Let us also add that the additional non-monotonicity near zero-entanglement that we had observed in the two-qubit clean case, is absent here in the three-qubit one. We believe that the reason is that the volume of separable states within the set of all quantum states (density matrices) decreases with increase in the number of parties [38, 68, 69], and references therein.

4. Conclusion

We have analyzed the response to introduction of disorder in multiparty quantum state parameters on the entanglement in those states. We have considered two-qubit and three-qubit states in the analysis, with the entanglement measure considered for two-qubit states being the concurrence and that for three-qubit states being the Jungnitsch–Moroder–Gühne genuine multiparty entanglement monotone. The relative frequency percentages of states for given (small) windows of entanglement are not uniform for all ranges of the entanglements. We measured this non-uniformity by the standard deviation of the entanglement distribution of these percentages. We found that insertion of disorder in the state parameters generically shrinks the standard deviation from its clean-case value (i.e. value in the corresponding case without disorder).

We began with Gaussian disorder in a single state parameter for two-qubit pure states, and found that the distribution of the disorder averaged entanglements has a lower standard deviation than the clean case. We then removed the specificities in this case in several ways. We considered non-Gaussian cases, viz when disorder is introduced by using the uniform distribution as well as that using the Cauchy–Lorentz one, where the latter one is different from the Gaussian and uniform distributions in that it does not have a mean. The Cauchy–Lorentz distribution turned out to be the one that provided the most hindrance to the spread of entanglement. We also considered the case when disorder is introduced in several state parameters, with more hindrance obtained as we increased the number of parameters in which disorder is inserted. We also found that increasing the strength of the disorder increases the localization effect on the entanglement spread.

We also considered the response of disorder introduction in parameters of three-qubit pure states, and found that the inhibition of the spread of entanglement—genuine multiparty entanglement in this case—can again be seen in this case. For both two- and three-qubit cases, we considered the effect of noise on the phenomenon of inhibition of spread of entanglement in response to disorder introduction.

Why does an entanglement measure that is allowed to span over a certain range does not cover that uniformly? The answer could be because the physical characteristic, viz entanglement, is a nonlinear function of the state parameters. A peak develops in the allowed range of entanglement, when random quantum states are chosen. The distribution therefore has an average, and a nontrivial spread. It may intuitively seem that if we perturb the state parameters, the distribution of the entanglement will also be perturbed: the mean will change and the spread will increase. What we saw is that while the mean does often change, the exact opposite happens for the spread: it decreases. Moreover, the stronger the perturbation, the stronger is the decrease in spread. This phenomenon can be understood by referring to how the behavior of entanglement of a quantum state depends on its entanglement content, when perturbed. We performed this analysis for sets of two-qubit pure states having different amounts of entanglement—with finite precision—and when the disorder is inserted in a single state parameter and, separately, in four parameters. We observed that when perturbed, there is a large probability for a state with an entanglement lower (higher) than the ‘average entanglement’ to jump to one with more (less) entanglement than in the parent state. Here, the average entanglement is the mean entanglement of Haar uniformly distributed states in the entire relevant Hilbert space. And this leads to a clustering effect, driving the disorder-affected system to have a low dispersion in the entanglement distribution. We believe that the results will be of importance for considerations in quantum technologies as well as for understanding the black hole information paradox.

Acknowledgments

US acknowledges partial support from the Department of Science and Technology, Government of India through the QuEST Grant (Grant No. DST/ICPS/QUST/Theme-3/2019/120).

Data availability statement

All data that support the findings of this study are included within the article (and any supplementary files).

ORCID iDs

George Biswas https://orcid.org/0000-0002-8929-0299
Anindya Biswas https://orcid.org/0000-0003-0078-5277
Ujjwal Sen https://orcid.org/0000-0002-0091-5847

References

[1] Emerson J, Weinstein Y S, Saraceno M, Lloyd S and Cory D G 2003 Pseudo-random unitary operators for quantum information processing *Science* **302** 2098
[2] Harrow A, Hayden P and Leung D 2004 Superdense coding of quantum states *Phys. Rev. Lett.* **92** 187901
[3] Hayden P, Leung D, Shor P W and Winter A 2004 Randomizing quantum states: constructions and applications *Commun. Math. Phys.* **250** 371
[4] Clowers B H, Belov M E, Prior D C, Danielson W F, Ibrahim Y and Smith R D 2008 Pseudorandom sequence modifications for ion mobility orthogonal time-of-flight mass spectrometry *Anal. Chem.* **80** 2464
[5] Ma X, Yuan X, Cao Z, Qi B and Zhang Z 2016 Quantum random number generation *npj Quantum Inf.* **2** 16021
[6] Russell N J, Chakhmakhchyan L, O'Brien J L and Laing A 2017 Direct dialling of Haar random unitary matrices *New J. Phys.* **19** 033007
[7] Muraleedharan G, Miyake A and Deutsch I H 2019 Quantum computational supremacy in the sampling of bosonic random walkers on a one-dimensional lattice *New J. Phys.* **21** 055003
[8] Preskill J 1998 *Lecture Notes for Physics 229: Quantum Information and Computation* (California: California Institute of Technology) https://www.lorentz.leidenuniv.nl/quantumcomputers/literature/preskill_1_to_6.pdf
[9] Nielsen M A and Chuang I L 2010 *Quantum Computation and Quantum Information* 10th edn (Cambridge: Cambridge University Press)
[10] Horodecki R, Horodecki P, Horodecki M and Horodecki K 2009 Quantum entanglement *Rev. Mod. Phys.* **81** 865
[11] Gühne O and Tóth G 2009 Entanglement detection *Phys. Rep.* **474** 1
[12] Das S, Chanda T, Lewenstein M, Sanpera A, Sen De A and Sen U 2016 The separability versus entanglement problem *Quantum Information* (New York: Wiley) ch 8 pp 127–74
[13] Page D N 1993 Average entropy of a subsystem *Phys. Rev. Lett.* **71** 1291
[14] Foong S K and Kanno S 1994 Proof of Page's conjecture on the average entropy of a subsystem *Phys. Rev. Lett.* **72** 1148
[15] Sen S 1996 Average entropy of a quantum subsystem *Phys. Rev. Lett.* **77** 1
[16] Smith G and Leung D 2006 Typical entanglement of stabilizer states *Phys. Rev.* A **74** 062314
[17] Dahlsten O C O, Oliveira R and Plenio M B 2007 The emergence of typical entanglement in two-party random processes *J. Phys. A: Math. Theor.* **40** 8081
[18] Serafini A, Dahlsten O C O, Gross D and Plenio M B 2007 Canonical and micro-canonical typical entanglement of continuous variable systems *J. Phys. A: Math. Theor.* **40** 9551
[19] Nakata Y and Murao M 2011 Simulating typical entanglement with many-body Hamiltonian dynamics *Phys. Rev.* A **84** 052321
[20] Müller M P, Dahlsten O C O and Vedral V 2012 Unifying typical entanglement and coin tossing: on randomization in probabilistic theories *Commun. Math. Phys.* **316** 441
[21] Deelan Cunden F, Facchi P, Florio G and Pascazio S 2013 Typical entanglement *Eur. Phys. J. Plus* **128** 48
[22] Dahlsten O C O, Lupo C, Mancini S and Serafini A 2014 Entanglement typicality *J. Phys. A: Math. Theor.* **47** 363001
[23] Fukuda M and Koenig R 2019 Typical entanglement for Gaussian states *J. Math. Phys.* **60** 112203
[24] Gentle J, Härdle W K and Mori Y 2012 *Handbook of Computational Statistics: Concepts and Methods* (Berlin: Springer)
[25] Einstein A, Podolsky B and Rosen N 1935 Can quantum-mechanical description of physical reality be considered complete? *Phys. Rev.* **47** 777
[26] Schrödinger E 1935 Discussion of probability relations between separated systems *Math. Proc. Camb. Phil. Soc.* **31** 555–63
[27] Werner R F 1989 Quantum states with Einstein–Podolsky–Rosen correlations admitting a hidden-variable model *Phys. Rev.* A **40** 4277
[28] Hill S and Wootters W K 1997 Entanglement of a pair of quantum bits *Phys. Rev. Lett.* **78** 5022
[29] Wootters W K 1998 Entanglement of formation of an arbitrary state of two qubits *Phys. Rev. Lett.* **80** 2245
[30] Jungnitsch B, Moroder T and Gühne O 2011 Taming multiparticle entanglement *Phys. Rev. Lett.* **106** 190502
[31] Press W H, Teukolsky S A, Vetterling W T and Flannery B P 1992 *Numerical Recipes in C: The Art of Scientific Computing* 2nd edn (Cambridge: Cambridge University Press)
[32] Bengtsson I and Zyczkowski K 2006 *Geometry of Quantum States: An Introduction to Quantum Entanglement* (Cambridge: Cambridge University Press)
[33] Cohn D 2013 *Measure Theory* 2nd edn (New York: Springer)
[34] Bennett C H, Bernstein H J, Popescu S and Schumacher B 1996 Concentrating partial entanglement by local operations *Phys. Rev.* A **53** 2046
[35] Bennett C H, DiVincenzo D P, Smolin J A and Wootters W K 1996 Mixed-state entanglement and quantum error correction *Phys. Rev.* A **54** 3824
[36] Peres A 1996 Separability criterion for density matrices *Phys. Rev. Lett.* **77** 1413
[37] Horodecki M, Horodecki P and Horodecki R 1996 Separability of mixed states: necessary and sufficient conditions *Phys. Lett.* A **223** 1
[38] Życzkowski K, Horodecki P, Sanpera A and Lewenstein M 1998 Volume of the set of separable states *Phys. Rev.* A **58** 883
[39] Lee J, Kim M S, Park Y J and Lee S 2000 Partial teleportation of entanglement in a noisy environment *J. Mod. Opt.* **47** 2151

[40] Vidal G and Werner R F 2002 Computable measure of entanglement *Phys. Rev.* A **65** 032314
[41] Plenio M B 2005 Logarithmic negativity: a full entanglement monotone that is not convex *Phys. Rev. Lett.* **95** 090503
[42] Chruściński D and Sarbicki G 2014 Entanglement witnesses: construction, analysis and classification *J. Phys. A: Math. Theor.* **47** 483001
[43] Vandenberghe L and Boyd S 1996 Semidefinite programming *SIAM Rev.* **38** 49
[44] Jungnitsch B 2011 PPTMixer: a tool to detect genuine multipartite entanglement http://mathworks.com/matlabcentral/fileexchange/30968
[45] Chowdhury D 1986 *Spin Glasses and Other Frustrated Systems* (Singapore: World Scientific)
[46] Mezard M, Parisi G and Virasoro M 1986 *Spin Glass Theory and Beyond* (Singapore: World Scientific)
[47] Chakrabarti B K, Dutta A and Sen P 1996 *Quantum Ising Phases and Transitions in Transverse Ising Models* 1st edn (Berlin: Springer)
[48] Nishimori H 2001 *Statistical Physics of Spin Glasses and Information Processing: An Introduction* (Oxford: New York: Oxford University Press)
[49] Sachdev S 2011 *Quantum Phase Transitions* 2nd edn (Cambridge: Cambridge University Press)
[50] Suzuki S, Inoue J and Chakrabarti B K 2013 *Quantum Ising Phases and Transitions in Transverse Ising Models* 2nd edn (Berlin: Springer)
[51] Saha T and Mookerjee A 1994 A study of annealed and quenched averaging of the thermodynamic potential in a disordered system: an augmented space approach *J. Phys.: Condens. Matter* **6** 1529
[52] Liu T and Bundschuh R 2005 Quantification of the differences between quenched and annealed averaging for RNA secondary structures *Phys. Rev.* E **72** 061905
[53] Blavatska V 2013 Equivalence of quenched and annealed averaging in models of disordered polymers *J. Phys.: Condens. Matter* **25** 505101
[54] von Hippel P 2011 Skewness *International Encyclopedia of Statistical Science* (Berlin: Springer) pp 1340–2
[55] Westfall P H 2014 Kurtosis as peakedness, 1905–2014. R.I.P *Am. Stat.* **68** 191
[56] Miszczak J A 2012 Generating and using truly random quantum states in mathematica *Comput. Phys. Commun.* **183** 118
[57] Życzkowski K, Penson K A, Nechita I and Collins B 2011 Generating random density matrices *J. Math. Phys.* **52** 062201
[58] Enríquez M, Delgado F and Życzkowski K 2018 Entanglement of three-qubit random pure states *Entropy* **20** 745
[59] Singh U, Zhang L and Pati A K 2016 Average coherence and its typicality for random pure states *Phys. Rev.* A **93** 032125
[60] Zyczkowski K and Sommers H-J 2001 Induced measures in the space of mixed quantum states *J. Phys. A: Math. Gen.* **34** 7111
[61] Sen(De) A and Sen U 2010 Channel capacities versus entanglement measures in multiparty quantum states *Phys. Rev.* A **81** 012308
[62] Sen(De) A and Sen U 2010 Bound genuine multisite entanglement: detector of gapless-gapped quantum transitions in frustrated systems (arXiv:1002.1253)
[63] Biswas A, Prabhu R, Sen(De) A and Sen U 2014 Genuine-multipartite-entanglement trends in gapless-to-gapped transitions of quantum spin systems *Phys. Rev.* A **90** 032301
[64] Das T, Roy S S, Bagchi S, Misra A, Sen(De) A and Sen U 2016 Generalized geometric measure of entanglement for multiparty mixed states *Phys. Rev.* A **94** 022336
[65] Shimony A 1995 Degree of entanglementa *Ann. New York Acad. Sci.* **755** 675
[66] Wei T-C and Goldbart P M 2003 Geometric measure of entanglement and applications to bipartite and multipartite quantum states *Phys. Rev.* A **68** 042307
[67] Blasone M, Dell'Anno F, De Siena S and Illuminati F 2008 Hierarchies of geometric entanglement *Phys. Rev.* A **77** 062304
[68] Życzkowski K 1999 Volume of the set of separable states. II *Phys. Rev.* A **60** 3496
[69] Szarek S J 2005 Volume of separable states is super-doubly-exponentially small in the number of qubits *Phys. Rev.* A **72** 032304